

Molecular Mechanisms of Yeast Cell Wall Glucan Remodeling*

Received for publication, October 17, 2008, and in revised form, December 19, 2008 Published, JBC Papers in Press, December 19, 2008, DOI 10.1074/jbc.M807990200

Ramon Hurtado-Guerrero^{‡1}, Alexander W. Schüttelkopf[‡], Isabelle Mouyna[§], Adel F. M. Ibrahim[¶], Sharon Shepherd[‡], Thierry Fontaine[§], Jean-Paul Latgé[§], and Daan M. F. van Aalten^{‡2}

From the [‡]Division of Biological Chemistry and Drug Discovery, College of Life Sciences, University of Dundee, Dundee DD1 5EH, Scotland, United Kingdom, the [¶]CLS DNA Manipulation Team, Division of Signal Transduction Therapy, College of Life Sciences, University of Dundee, Dundee DD1 5EH, Scotland, United Kingdom, and the [§]Unité des Aspergillus, Institut Pasteur, Paris 75724, France

Yeast cell wall remodeling is controlled by the equilibrium between glycoside hydrolases, glycosyltransferases, and transglycosylases. Family 72 glycoside hydrolases (GH72) are ubiquitous in fungal organisms and are known to possess significant transglycosylase activity, producing elongated $\beta(1-3)$ glucan chains. However, the molecular mechanisms that control the balance between hydrolysis and transglycosylation in these enzymes are not understood. Here we present the first crystal structure of a glucan transglycosylase, *Saccharomyces cerevisiae* Gas2 (*ScGas2*), revealing a multidomain fold, with a $(\beta\alpha)_8$ catalytic core and a separate glucan binding domain with an elongated, conserved glucan binding groove. Structures of *ScGas2* complexes with different β -glucan substrate/product oligosaccharides provide “snapshots” of substrate binding and hydrolysis/transglycosylation giving the first insights into the mechanisms these enzymes employ to drive $\beta(1-3)$ glucan elongation. Together with mutagenesis and analysis of reaction products, the structures suggest a “base occlusion” mechanism through which these enzymes protect the covalent protein-enzyme intermediate from a water nucleophile, thus controlling the balance between hydrolysis and transglycosylation and driving the elongation of $\beta(1-3)$ glucan chains in the yeast cell wall.

The cell wall of fungal organisms is a dynamic structure, providing protection against hostile environments, yet also harboring many hydrolytic and toxic molecules required for the fungus to invade its ecological niche (1). Polysaccharides account for over 90% of the cell wall. The central skeletal component of the cell wall common to the vast majority of fungal species is a branched core of $\beta(1,3)$ glucan, linked to chitin via a $\beta(1,4)$ linkage (1). Interchain $\beta(1,6)$ glucosidic linkages account for 3 and 4% of the total glucan linkages in *Saccharomyces cerevisiae* and *Aspergillus fumigatus*, respectively (2–4). This core is

embedded in a complex of amorphous proteins and/or polysaccharide whose composition is highly species-dependent. The core $\beta(1,3)$ glucan is subjected to continuous synthetic elaboration, degradation, and remodeling by a large arsenal of enzymes, whose activities must be appropriately balanced to provide the cell wall with adequate elasticity to allow growth, budding, or branching and yet sufficient strength to guard against cell lysis (1).

Glucan synthase is a protein complex located at the plasma membrane, synthesizing $\beta(1,3)$ glucan from UDP-glucose (65–90% of the total glucan). In cell wall remodeling, glycoside hydrolases and glycosyltransferases/transglycosylases play a crucial role (1, 5). Pure glycoside hydrolases degrade glycans mainly to regulate the plasticity of the cell wall under different circumstances, such as cell division, cell separation, and sporulation (5), whereas glycoside hydrolases with significant transglycosylase activity are capable of forming new glycosidic bonds between oligosaccharides, generating longer or branched polymers. Previous studies have shown that several proteins anchored to the plasma membrane by a glycosylphosphatidylinositol (GPI)³ anchor have transglycosylase activities (6–10). Among them are the Gas (in *S. cerevisiae*)/Gel (in *A. fumigatus*) proteins that belong to the GH72 family in the CAZy data base (11). For laminarioligosaccharides with >10 sugars, these enzymes are able to cleave a $\beta(1-3)$ bond and transfer the newly formed reducing end (the “donor”) to the nonreducing end of another oligosaccharide (the “acceptor”) (6, 12, 13). This transferase reaction generates a new $\beta(1,3)$ linkage, resulting in the elongation of $\beta(1,3)$ glucan chains, offering a mechanism for the synthesis of longer glucan chains as alternative to, or in synergy with, glucan synthase. The Gas/Gel proteins consist of a signal sequence, a catalytic core, and either a cysteine-rich domain (classified as a carbohydrate-binding module, CBM43) (11) or a Ser-Thr-rich motif, followed by a GPI anchor (Fig. 1A). Based on the presence or absence of the C-terminal cysteine-rich domain, the family is subdivided into GH72⁺ (with a CBM43 domain) and GH72⁻ (without a CBM43 domain) (14). The genome of *S. cerevisiae* contains five proteins (Gas1–Gas5), two of which (Gas1 and Gas2) belong to the GH72⁺ subfamily. With the exception of Gas3, transglycosylase activity has been reported for all these enzyme (14, 15). *A. fumigatus* contains seven genes (*gel1–gel7*), with only Gel1p, Gel2p (both GH72⁻), and Gel4p (GH72⁺) being expressed during mycelial growth in

* This work was supported by a Wellcome Trust senior research fellowship (to D. M. F. v. A.) and European Union FP6 STREP Fungwall Programme. The costs of publication of this article were defrayed in part by the payment of page charges. This article must therefore be hereby marked “advertisement” in accordance with 18 U.S.C. Section 1734 solely to indicate this fact. The atomic coordinates and structure factors (codes 2W61, 2W62, and 2W63) have been deposited in the Protein Data Bank, Research Collaboratory for Structural Bioinformatics, Rutgers University, New Brunswick, NJ (<http://www.rcsb.org/>).

¹ To whom correspondence may be addressed. Fax: 44-1382 385764; E-mail: R.Hurtadoguerrero@dundee.ac.uk.

² To whom correspondence may be addressed. Fax: 44-1382 385764; E-mail: dmfvanaalten@dundee.ac.uk.

³ The abbreviations used are: GPI, glycosylphosphatidylinositol; CTD, C-terminal domain; PDB, Protein Data Bank; r.m.s.d., root mean square deviation.

rich media (12). In *Candida albicans* five GH72 enzymes, PHR1–3 (known as pH-regulated enzymes) and PGA4–5, have been detected. PHR1, PHR2, and PGA5 belong to GH72⁺, whereas PHR3 and PGA4 belong to the GH72⁻ subfamily. It was shown that all these proteins, irrespectively of the presence/absence of a CBM43 domain, display the same glycosyltransferase activity (14).

The essential function of these enzymes in fungal morphogenesis has been shown by gene disruption studies in a number of organisms. For instance, a gene knock-out of *Scgas1* led to aberrant cell morphology, reduced growth rate, cell aggregation, and different cell wall composition (16, 17). A double knock-out of *Scgas2* and *Scgas4* showed a severe reduction in the efficiency of sporulation, an increased permeability of the spores to exogenous substances, and production of unviable spores (15). Single and double knockouts of *Afge12* and double knockouts of *Afge11/Afge12* resulted in slower growth, abnormal conidiogenesis, and an altered cell wall composition (12). *Caphr1* and *Caphr2* single knock-outs show defects in growth and morphogenesis, reduction in $\beta(1,3)$ glucan-associated $\beta(1,6)$ glucans, and a 5-fold increase in the chitin content of the walls (18–20).

Despite considerable interest in the molecular mechanisms of these transglycosylases, it is currently not understood what structure these enzymes adopt, how they interact with the substrate, what mechanism they adopt for the initial nucleophilic attack, and crucially, how they are able to drive the reaction toward transglycosylation and not hydrolysis in the presence of a high concentration of a more available nucleophile, water.

Here we present the first crystal structure of a GH72⁺ glucanosyltransferase enzyme, *ScGas2*, in complex with laminari-pentaose and a complex with the hydrolysis products of laminariheptaose. The crystal structure reveals a $(\beta\alpha)_8$ catalytic core, tightly interacting with the C-terminal CBM43 glucan binding domain. The active site is located in an unusual tyrosine-rich groove, possessing two glutamic acids as catalytic residues. Site-directed mutagenesis data together with crystal structures of the *ScGas2*-oligosaccharide complexes shows that product binding in the acceptor site is crucial for tuning the balance between hydrolysis and transglycosylation.

EXPERIMENTAL PROCEDURES

Cloning, Expression, and Purification—The DNA sequence encoding amino acid residues 26–525 of the *S. cerevisiae ScGas2* (Swiss-Prot, locus *ScGas2_YEAST*; Swiss-Prot accession number Q06135; GeneID, 851056), defined as *scgas2*, was obtained by PCR from *S. cerevisiae* strain W303 genomic DNA, using the forward primer, 5'-ATCTCGAGAA-AAGAGAGGCTGAAGCTTCAGGTGTCAGCTTTGAAAA-AACCCCTG, containing a recognition sequence for XhoI (underlined) and a KEX2 cleavage signal (italic), and the reverse primer, 5'-GCTCTAGACTAACTCGATGGGTACTTTACG-TTCAAATTTCC-3', containing a recognition sequence for XbaI (underlined), and cloned into the pSC-B vector (Stratagene). Following digestion with XhoI and XbaI, the cloned sequence was subcloned into the *Pichia pastoris* protein expression and secretion vector pPICZ α A (Invitrogen), resulting in the expression plasmid pPICZ α Scgas2 (Ser²⁶–Ser⁵²⁵). Subsequently, the

codons for the asparagine residues at positions 498 and 510 in *ScGas2* were simultaneously changed by site-directed mutagenesis to aspartic acid codons (removing N-linked glycosylation sites) using the forward primer, 5'-GAATGTTTT-TGATTCTATAAGGGATATCACATACAATCATGGCGAT-TATTC-3', and the reverse primer, 5'-CTTTCCTTGCTA-CGCGATGGATCTGATTTTGAATAATCGCCATG-3'.

The resulting plasmid, pPICZ α Agas2 (Ser²⁶–Ser⁵²⁵) N498D/N510D, referred to here as the wild type, was used as template for introducing the following single amino acid changes by site-directed mutagenesis as follows: Q62A, Y107F, Y107Q, D132N, N175A, E176Q, Y244F, Y244Q, E275Q, Y307Q, F404A, and Y474A, such that each of the resulting 12 plasmids carried the indicated mutation in addition to the previously introduced asparagine to aspartic acid mutations at positions 498 and 510. Site-directed mutagenesis was carried out following the QuikChange protocol (Stratagene), using the KOD HotStart DNA polymerase (Novagene). All plasmids were verified by sequencing (DNA Sequencing Service, College of Life Sciences, University of Dundee, Scotland, UK).

All plasmids were isolated from *Escherichia coli* strain DH5 α , linearized with PmeI, and used to transform *P. pastoris* strain into X-33 following the LiCl method (Invitrogen) or using the *Pichia EasyComp*TM transformation kit (Invitrogen). Transformants were selected on YPD plates (1% (w/v) yeast extract, 2% (w/v) peptone, 2% (w/v) dextrose) containing 100 μ g/ml Zeocin (Invitrogen). Batch cultures were performed in a 100-ml volume of BMGY medium (1% (w/v) yeast extract, 2% (w/v) peptone, 100 mM potassium phosphate (pH 6.0), 1.34% (w/v) yeast nitrogen base, and 1% (v/v) glycerol). 50 ml were used to grow 500 ml of BMGY medium overnight at 30 °C, and expression was induced by methanol (1%, v/v) for 72 h at room temperature in a shaking incubator (270 rpm). Yeast cells were harvested by centrifugation at 3480 $\times g$ for 30 min. The supernatants containing soluble *ScGas2* were filtered to 0.2 μ m, concentrated to 50 ml using a Vivaflow 200 cassette (10,000 M_r weight cutoff, PES membrane; Vivascience), and dialyzed against water.

The samples were then loaded onto a 2 \times 5-ml HiTrap Q FF column (Amersham Biosciences) that had been equilibrated with 10 column volumes of 25 mM Tris, pH 7.0, on an AKTA purifier system. Following loading, the column was washed with 10 column volumes of 25 mM Tris, pH 7.0. The protein was eluted with a salt gradient (0–500 mM NaCl) over 20 column volumes, collecting 2-ml fractions. The fractions containing the proteins were then pooled and concentrated to 5 ml using Vivaspin 10,000 M_r weight cutoff. Subsequently, gel filtration was carried out using a Superdex 75 XK26/60 column in 25 mM Tris, 150 mM NaCl, pH 7.0. The concentrated *ScGas2* proteins were used for both kinetic analysis and crystallization trials.

Enzymology—To test for $\beta(1,3)$ glucanosyltransferase/hydrolyase activity, the purified proteins (10 μ g) were incubated with the linear reduced laminarioligosaccharides rG5, rG7, and rG19 at a concentration of 4 mM in 50 mM sodium acetate buffer, pH 5.5, at 37 °C. Aliquots of 2.5 μ l were withdrawn at different times (0, 1, and 3 h and overnight), supplemented with 47.5 μ l of 50 mM NaOH, and then analyzed by high performance anion-exchange chromatography through a CarboPAC-

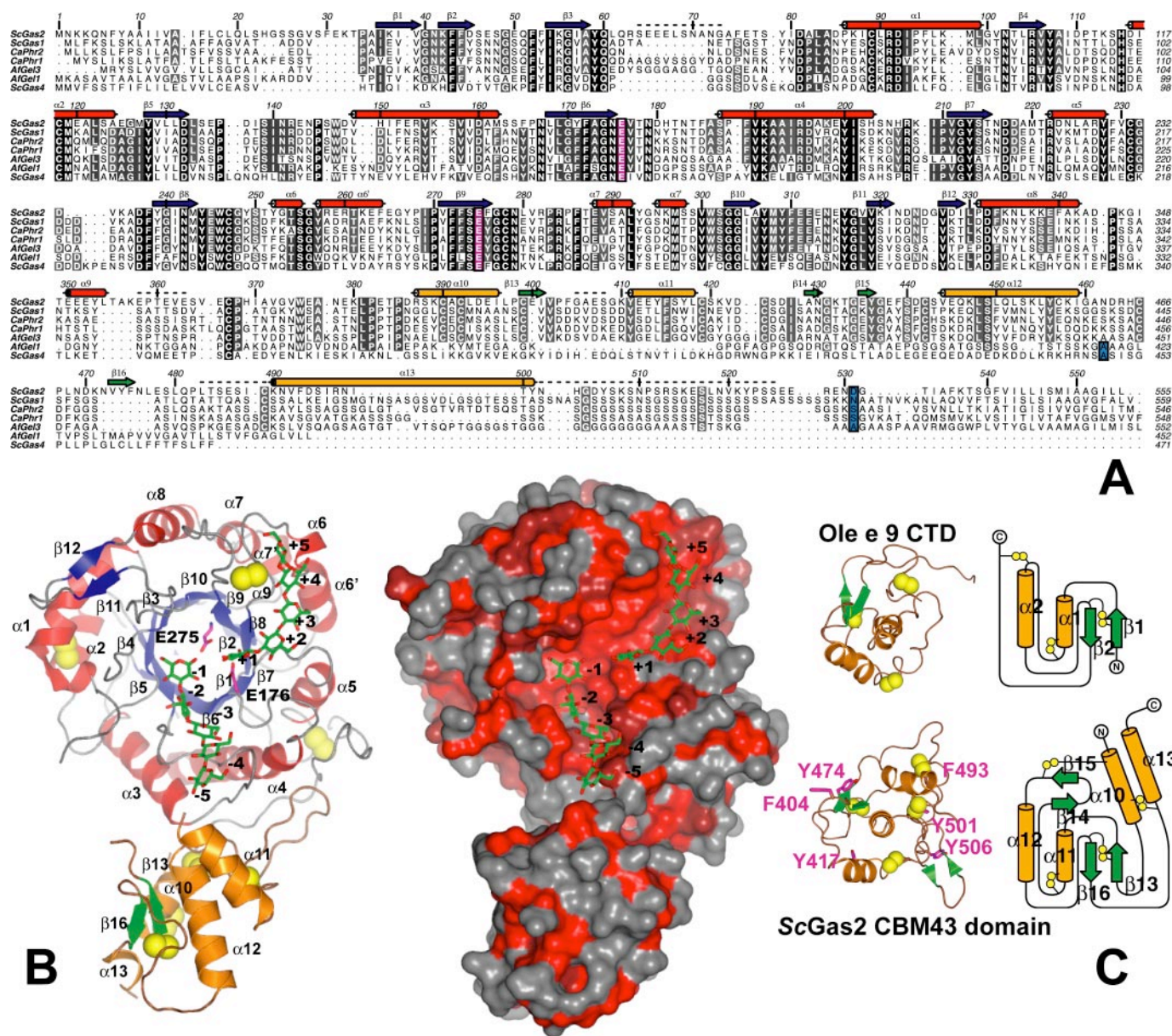


FIGURE 1. Overall structure of ScGas2 and comparison with structurally related proteins. *A*, multiple sequence alignment of the GH72 family members ScGas2, ScGas1, CaPhr2, CaPhr1, AfGel3, AfGel1, and ScGas4. Secondary structure elements from the ScGas2 structure are shown, with α -helices in red and orange for the catalytic and cysteine-rich domains, respectively, and β -strands correspondingly in blue and green. Regions that are disordered in some or all of the ScGas2 structures are marked with a dashed line. Conserved catalytic glutamate residues are highlighted in pink boxing, and the (predicted) GPI-anchor attachment site is indicated in blue boxing. *B*, overall crystal structure of ScGas2 in complex with laminaripentaose. The Glu¹⁷⁶ and Glu²⁷⁵ are shown with pink carbon atoms and labeled. The seven disulfide bridges are highlighted in yellow. Helix α 13 was not built in the laminaripentaose complex structure and thus is absent from this figure. Ligand molecules are shown as sticks with green carbon atoms and the sugar-binding sites are labeled -5 to +5, following standard nomenclature. Other colors as in *A*. Also shown is a surface representation of the ScGas2, colored by sequence conservation (red (100% identity) to gray (<50% identity)). *C*, comparison of the CBM43 domains of ScGas2 (bottom; E176Q mutant) and Ole e 9 (top; PDB ID 2JON (39)). Disulfide bridge sulfur atoms are shown as yellow spheres. Secondary structure elements are colored as in *B* and labeled. Unique features of either structure are shown in lighter colors in the picture (left). The topology diagram was drawn with Topdraw (50). Surface-exposed aromatic amino acids of the CBM43 domain of ScGas2 (Phe⁴⁰⁴, Tyr⁴¹⁷, Tyr⁴⁷⁴, Phe⁴⁹³, Tyr⁵⁰¹, and Tyr⁵⁰⁶) are shown as sticks with pink carbon atoms.

PA1 column (Dionex 4.6 mm inner diameter \times 250 mm), as described by Hartland *et al.* (21).

Crystallization and Data Collection—ScGas2 was spin-concentrated to 21 mg/ml. Crystals were grown by sitting drop experiments at 20 °C through mixing 1 μ l of protein with an equal volume of a reservoir solution (20% 1,4-butanediol, 5% acetone, 0.1 M sodium acetate, pH 4.5). Under these conditions, crystals appeared within 3–7 days. They were cryoprotected

with 0.1 M sodium acetate, 30% 1,4 butanediol, 5% acetone, pH 4.5, and flash-cooled prior to data collection at 100 K.

(NH₄)₃IrCl₆ derivative, as well as oligosaccharide complexes, were generated by soaking apo-crystals in cryoprotectant supplemented with heavy atom salt (10–100 mM), laminaripentaose (200 mM), or laminariheptaose (100 mM), respectively, for 10–20 min prior to data collection. Data for heavy atom derivative was collected at beamline ID23-2 (ESRF, Grenoble,

TABLE 1
Data collection and refinement statistics

Values in parentheses refer to the highest resolution shell. Ramachandran plot statistics were determined with PROCHECK (29). NA means not applicable.

	E176Q apo-structure	(NH ₄) ₃ IrCl ₆ derivative	Laminaripectose complex	Laminariheptaose complex
Wavelength	0.912 Å	0.873 Å	1.54 Å	1.54 Å
Resolution	20.00 to 1.62 Å (1.68 to 1.62 Å)	25.00 to 2.10 Å (2.15 to 2.10 Å)	20.00 to 1.85 Å (1.92 to 1.85 Å)	20.00 to 1.90 Å (1.92 to 1.85 Å)
Cell dimensions	<i>a</i> = 051.88, <i>b</i> = 064.48, <i>c</i> = 152.04 Å	<i>a</i> = 050.37, <i>b</i> = 070.57, <i>c</i> = 150.91 Å	<i>a</i> = 050.04, <i>b</i> = 070.84, <i>c</i> = 149.15 Å	<i>a</i> = 050.02, <i>b</i> = 070.27, <i>c</i> = 148.91 Å
Unique reflections	65,435	31,981	46,135	42,459
Completeness	98.2 (96.6)	99 (100)	99.7 (100)	94.7 (97.8)
<i>R</i> _{sym}	0.054 (0.250)	0.077 (0.162)	0.045 (0.293)	0.043 (0.228)
<i>I</i> / σ (<i>I</i>)	18.4 (4.1)	21.0 (10.9)	23.3 (5.5)	20.2 (5.7)
Redundancy	3.6 (2.9)	8.2 (8.1)	5.3 (5.2)	4.4 (4.2)
No. of protein residues	470		436	432
No. of sugar residues	000		010	007
Solvent molecules	677		313	293
<i>R</i> _{work} / <i>R</i> _{free}	0.175/0.217		0.186/0.209	0.182/0.190
r.m.s.d. from ideal geometry, bonds	0.012 Å		0.012 Å	0.013 Å
r.m.s.d. from ideal geometry, angles	1.28°		1.33°	1.33°
Wilson <i>B</i>	28.3 Å ²	25.6 Å ²	37.4 Å ²	38.5 Å ²
$\langle B \rangle$ overall	27.9 Å ²		42.4 Å ²	41.2 Å ²
$\langle B \rangle$ ligand	NA		44.7 Å ²	54.1 Å ²
$\langle B \rangle$ solvent	32.1 Å ²		45.1 Å ²	44.1 Å ²
Ramachandran plot				
Most favored	90.3%		91.1%	90.2%
Additionally allowed	9.5%		8.9%	9.8%
Generously allowed	0.2%		0.0%	0.0%
PDB ID	2W61		2W62	2W63

TABLE 2
Percentage of degraded reduced G19 after 1 h of incubation of the ScGas2 mutants compared with the wild type enzyme. ND means not determined

ScGas2 (S26-S525)	Percentage of degraded G19	Transglycosylation product
		%
ScGas2 (wildtype)	93 ± 4	100
Q62A	88 ± 4	ND
Y107F	49 ± 2	20 ± 8
Y107Q	ND	ND
D132N	85 ± 4	ND
N175A	1 ± 2	ND
E176Q	1 ± 2	ND
Y244Q	39 ± 2	9 ± 7
Y244F	ND	ND
E275Q	1 ± 2	ND
Y307Q	33 ± 4	11 ± 2
F404A	49 ± 2	ND
Y474A	92 ± 4	100 ± 12

France), all other data were collected in-house on a Rigaku RU-200 rotating anode with an R-AXIS IV detector. All data were processed and scaled using the HKL suite (22) and CCP4 software (23), relevant statistics are given in Table 1.

Structure Determination and Refinement—Using SHELXC/D/E we were able to find 14 ordered iridium sites. By SIRAS, using data from a crystal soaked with (NH₄)₃IrCl₆ as well as a data set on a crystal of the E176Q mutant (Table 1), an initial model for the apo-structure was generated with ARP/warp (25) (initially building 412 residues of the single protein monomer in the asymmetric unit) and improved through cycles of manual model building in Coot (26) and refinement with REFMAC5 (27). Molecular replacement with this structure as a search model was used to generate phases and starting models for the remaining data sets, which were refined similarly. Topologies for the oligosaccharide ligands were generated with PRODRG (28). The final models were validated with PROCHECK (29) and WHATCHECK (30), and model statistics are given in

Table 1. Coordinates and structure factors have been deposited in the Protein Data Bank. The structure has several disordered regions as follows: one in the poorly conserved loop between β 3 and α 1, one covering a short stretch of the interdomain region between α 9 and α 10, and one (absent in three of the present four structures) preceding α 11. In addition, the C terminus of ScGas2 (from at least Ser⁵⁰⁷, but in some cases as early as Leu⁴⁸³) is completely disordered. Although density for the α 13 helix could be observed in all three structures, its quality was too poor for it to be modeled in the oligosaccharide complexes (Fig. 1B).

RESULTS AND DISCUSSION

Structure of ScGas2 Reveals a Two-domain Fold—A truncated form of ScGas2 (amino acids 26–525, excluding the signal/GPI-anchor sequences, Fig. 1A) was expressed as a secreted protein in *P. pastoris* and purified by ion-exchange and gel filtration chromatography. The structure of ScGas2 was solved by SIRAS with an iridium derivative, complexes with laminarioligosaccharides and a structure of a E176Q mutant were solved by molecular replacement, and all structures were refined to 1.6–2.1 Å with *R*_{free} < 0.22 (Table 1).

The structure of ScGas2 is composed of two interacting domains as follows, a ($\beta\alpha$)₈ catalytic domain, abundantly found in other carbohydrate active enzymes; and a C-terminal cysteine-rich domain of the CBM43 family (11) (Fig. 1). The ($\beta\alpha$)₈ domain deviates from the canonical topology by kinks in the sixth and seventh α -helix (α 6/ α 6' and α 7/ α 7', Fig. 1A). Similar to many other ($\beta\alpha$)₈ barrel proteins, the first strand of the barrel (β 3) is preceded by a two-stranded antiparallel β -sheet, which seals the “bottom” of the barrel. A second short two-stranded sheet (β 11/ β 12) is inserted into the last $\beta\alpha$ loop (31), placing it on the opposite side of the barrel and within 20 Å of the active site (Fig. 1).

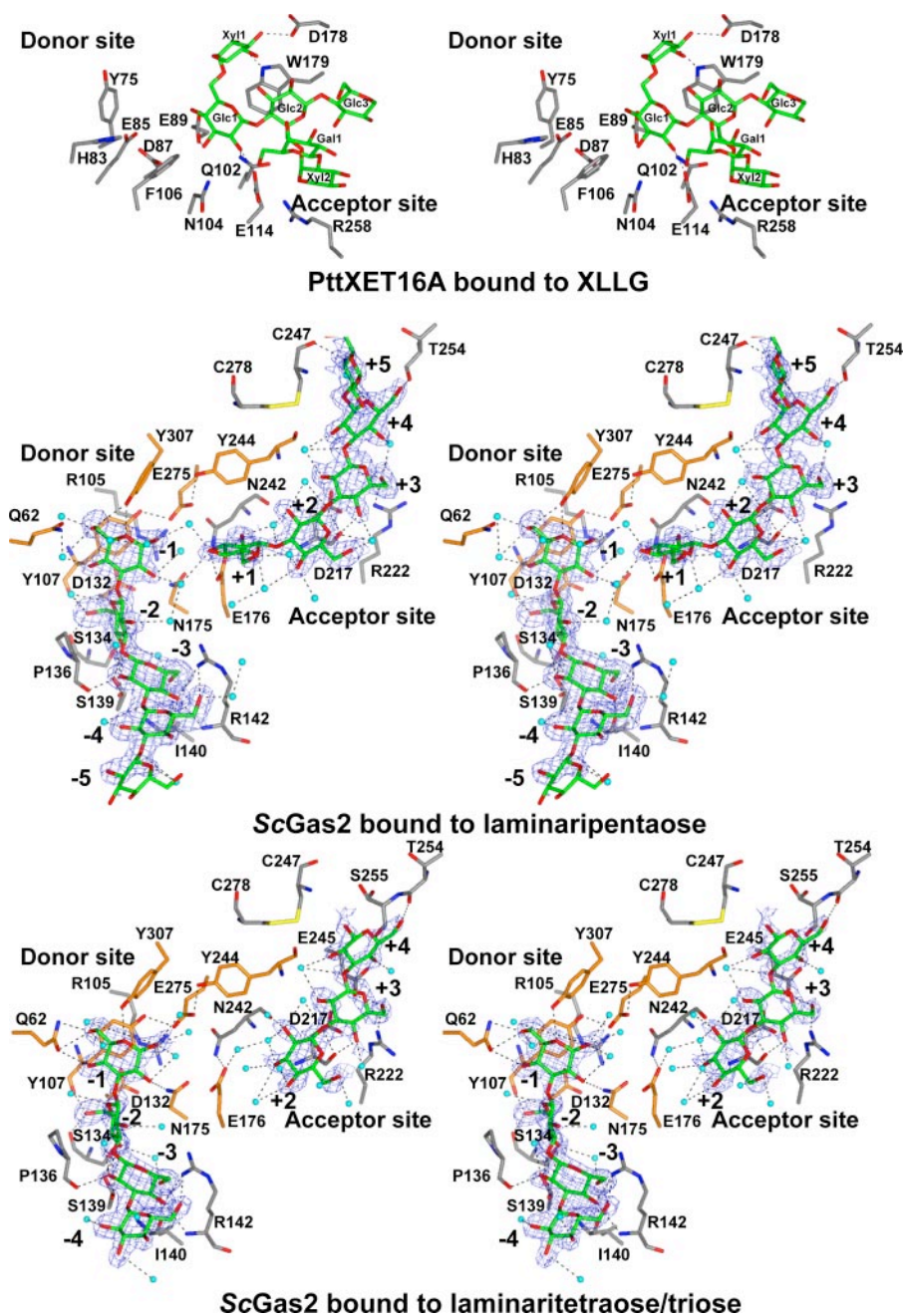


FIGURE 2. Structures of ScGas2-laminarioligosaccharide complexes. Stereo view of the active site of ScGas2 in complex with laminariipentaose and the hydrolysis products of laminariheptaose (*i.e.* laminaritetraose + laminaritriose), and comparison with PttXET16A bound to XLLG. The active site oriented to facilitate identification of the donor (*left*) and acceptor (*right*) subsites. The amino acids placed in the donor site and acceptor sites are shown as sticks with gray carbons. The residues targeted by site-directed mutagenesis, Gln⁶², Tyr¹⁰⁷, Asp¹³², Asn¹⁷⁵, Glu¹⁷⁶, Tyr²⁴⁴, Glu²⁷⁵, Tyr³⁰⁷, Phe⁴⁰⁴, and Tyr⁴⁷⁴, are shown with orange carbon atoms. XLLG, laminariipentaose, laminaritetraose, and laminaritriose are represented as stick models with green carbon atoms. Protein-ligand and water-ligand hydrogen bonds are shown as dotted black lines. Water molecules involved in hydrogen bonds with the ligands are shown as cyan spheres. For clarity purposes, protein-water hydrogen bonds are not shown. Unbiased (*i.e.* before inclusion of any ligand model) $|F_o| - |F_c|$, ϕ_{calc} electron density maps are shown at 2.5 σ .

Not surprisingly, a DALI (32) search with the ScGas2 catalytic domain yields over 300 proteins with significant structural similarity; among the most similar structures are numerous glucosidases. The two crystal structures with the highest Z scores are domain 3 from human β -glucuronidase (PDB ID 1BHG (33)) and *Cellvibrio mixtus* mannosidase 5A (PDB ID

1UUQ (34)), which superimpose with r.m.s.d. of 2.7 Å and 3.0 Å for ≈ 260 C- α atoms, respectively.

The ScGas2 catalytic domain contains three disulfide bridges, one between Cys⁸⁹ and Cys¹¹⁸ connecting $\alpha 1$ and $\alpha 2$, and another between Cys²³¹ from the fifth $\alpha\beta$ loop and Cys³⁶⁷ from the interdomain loop. It is noteworthy that both these disulfides occur in the vicinity of disordered loops, and it is possible that they help to limit flexibility. The third disulfide of the catalytic domain is formed by Cys²⁴⁷ and Cys²⁷⁸ from the sixth and seventh $\beta\alpha$ loop (preceding $\alpha 6$ and $\alpha 8$, respectively). Both these loops are involved in forming the acceptor saccharide-binding site, and it is possible that the disulfide bridge helps to correctly position them.

When a sequence alignment of GH72 enzymes (Fig. 1A) is interpreted in the context of the ScGas2 structure (Fig. 1B), it is clear that most of the sequence conservation locates to the catalytic core, whereas the C-terminal cysteine-rich CBM43 domain of ScGas2 is less conserved. In particular the active site of ScGas2 is highly conserved (Fig. 1B), from the -2 to the +2 site, suggesting that ScGas2 may be a good representative of the GH72 family for further mechanistic studies.

CBM43 Domain Contains a Conserved Cysteine Structure and Exposed Aromatic Residues—Based on its sequence, the C-terminal domain of ScGas2 (Fig. 1) has been assigned to the CBM43 family of carbohydrate-binding modules (11). It assumes a predominantly α -helical structure; a core formed by four α -helices is augmented by two small antiparallel two-stranded β -sheets (Fig. 1C). Although the amino acid sequence of the catalytic domain is reasonably well conserved among GH72 family mem-

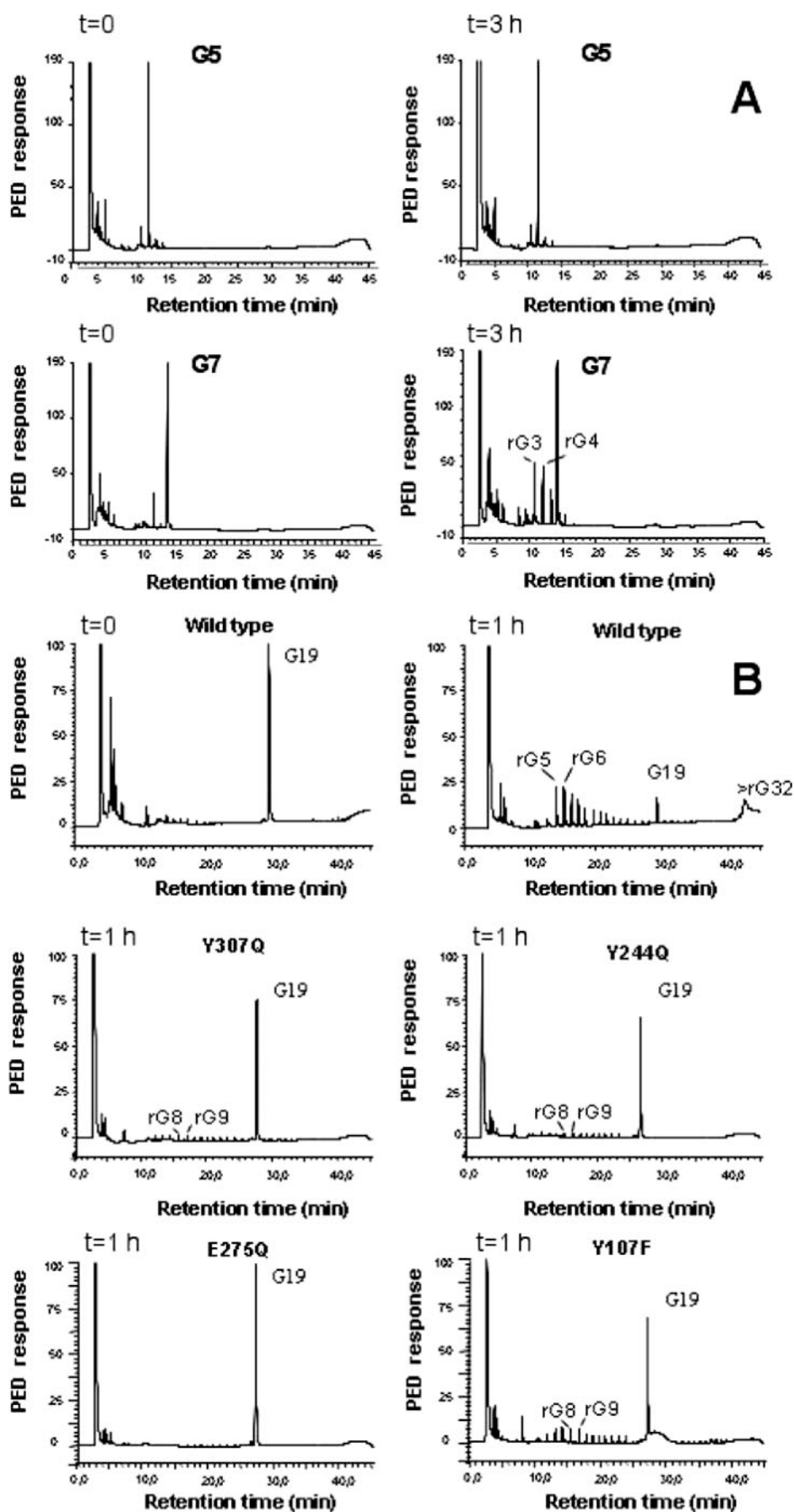
bers (32–61% identity), there is considerably more variation in the C-terminal domain, where, even among GH72⁺ subfamily members, sequence identity can drop below 20% (Fig. 1A). The few amino acids that are completely conserved include a number of hydrophobic residues and eight cysteines, which, in the ScGas2 structure, form four disulfide bridges (Cys³⁹⁰–Cys⁴⁴²;

Insights into Fungal Transglycosylation

Cys³⁹⁹–Cys⁴⁶⁶; Cys⁴¹⁹–Cys⁴²⁴; and Cys⁴⁵⁷–Cys⁴⁸⁹, Fig. 1, A–C), in agreement with a recent mass spectrometry-based assignment (35). The C-terminal ≈ 40 residues of the expressed protein, which in the full-length protein would lead up to the GPI anchor, are (mostly) disordered in our structures; it is likely that the poorly conserved stretch between $\alpha 15$ and the GPI anchor site functions as a flexible tether.

Structural homology searches of this domain with DALI (32) yielded no significant hits. As CBM43 domains are most commonly associated with $\beta(1,3)$ glucan-processing domains from CAZy families GH17/72, it is possible that they would possess $\beta(1,3)$ glucan binding activity. It has been shown that carbohydrate binding to CBM domains is generally effected by surface-exposed tyrosine, tryptophan, and phenylalanine residues (36). The *ScGas2* cysteine-rich domain contains six such surface aromatic amino acids: Phe⁴⁰⁴, Tyr⁴¹⁷, Tyr⁴⁷⁴, Phe⁴⁹³, Tyr⁵⁰¹, and Tyr⁵⁰⁶ (Fig. 1C), which could play a role binding to $\beta(1,3)$ glucan, although none of them are conserved between different GH72⁺ family members (Fig. 1A). To test this hypothesis, Phe⁴⁰⁴ and Tyr⁴⁷⁴ were mutated to alanines. Only the F404A mutant showed a small difference in transglycosylation/hydrolysis activity of a G19 laminarioligosaccharide compared with the wild type enzyme (Table 2). Earlier studies also showed that the presence or absence of the CBM43 domain in the GH72 enzymes does not appear to significantly affect transglycosylation activity (13, 14).

So far, only two CBM43 proteins, both olive pollen allergens, have been biochemically characterized in some detail. The olive pollen-derived Ole e 10 (an isolated CBM43 domain) and the GH17 family member Ole e 9 (with a C-terminal CBM43 domain) have been shown to possess the ability to bind β -1,3 glucan structures (37, 38). Although alignment between the olive pollen CBM43 domains and that of *ScGas2*



shows poor sequence conservation (identity of $\approx 17\%$), six of the GH72⁺ cysteines appear to be conserved. Very recently, an NMR structure of the C-terminal domain (CTD) of Ole e 9 has become available (39). A superposition with the ScGas2 cysteine-rich domain is relatively poor, giving an r.m.s.d. of 2.7 Å (with only 64 out of the 101 possible equivalenced C- α atoms; Fig. 1C). Although the two CBM43 structures share the “core” formed by $\alpha 11$, $\alpha 12$, $\beta 13$, and $\beta 16$ (ScGas2 numbering), the Ole e 9 CTD lacks the second β -sheet ($\beta 14$ – $\beta 15$) of ScGas2 as well as the $\alpha 10$ and $\alpha 13$ helices. Of the six equivalent cysteine residues, only four participate in structurally conserved disulfide bridges, whereas the other two form a third disulfide in the Ole e 9 CTD but participate in two separate disulfide bridges in ScGas2 (Fig. 1C). Altogether, the two available structures of CBM43 domains suggest that GH17-associated “plant” and GH72-linked “fungal” CBM43 domains, although sharing some structural motifs, are overall not similar enough that their functional equivalence can be assumed. Some of the ScGas2 structural elements absent from the Ole e 9 CTD participate in interactions with the catalytic domain (see below), and their absence from the plant protein may indicate differences in the interaction between the CBM and the two classes of catalytic domains. It is noteworthy that the part of the CBM43 domains incorporating the shared features is closest to the ScGas2 active site, whereas the dissimilar side faces away from it (Fig. 1B). It is thus possible that the CBMs of ScGas2 and Ole e 9 bind glucans on that side of the domain, using similar binding sites. Ole e 9 exposes a cluster of four surface aromatic residues on this side, most of which are conserved in Ole e 10 (39). Only one of these residues is conserved between Ole e 9 and ScGas2 (Tyr⁴¹⁷ in ScGas2 numbering).

One of the characteristics of CBM motifs/modules is that they are frequently separate domains and indeed can occur as individual proteins (40). In contrast, the cysteine-rich domain of ScGas2 shares extensive contacts with the catalytic core, incorporating hydrophobic interactions as well as seven strong direct hydrogen bonds and burying ≈ 2650 Å², compatible with a stable domain interface (41). The catalytic subunit contributes residues from around the N termini of helices $\alpha 3$ and $\alpha 4$ as well as the loop preceding $\alpha 10$ to the interface, whereas the CBM uses residues from the N-terminal ends of $\alpha 10$ and $\alpha 12$ and, most importantly, the small β -sheet formed by $\beta 14$ and $\beta 15$ that is absent from the Ole e 9 structure.

Binding Mode of a Transglycosylation Acceptor Substrate—Recent landmark studies toward the structure and mechanism of a plant xylosyltransferase PttXET16A has revealed how a large, fully ordered, oligosaccharide is bound to the acceptor site, tightly interacting with the catalytic base (Fig. 2), whereas elegant kinetic studies have demonstrated a remarkably long lived covalent enzyme-donor intermediate (42, 43).

To allow trapping of an ScGas2-acceptor transglycosylation complex, we sought to identify the minimal (and therefore most soluble) β -glucan-derived laminarioligosaccharide that would

not undergo hydrolysis, yet still serves as an acceptor substrate given a suitable donor in a transglycosylation reaction. Hydrolysis experiments show that laminaripentaose is not hydrolyzed by ScGas2 (Fig. 3A), although a previous study of the *A. fumigatus* Gel1 ScGas2 orthologue showed that laminaripentaose was the smallest laminarioligosaccharide acceptor used by the enzyme (21). Surprisingly, soaking experiments with ScGas2 revealed not only an ordered laminaripentaose bound to the acceptor site, but also a (noncovalently bound) laminaripentaose bound in the donor site (Fig. 2). The active site is defined by two catalytic residues, Glu¹⁷⁶ and Glu²⁷⁵, previously identified by mutagenesis (13), and three tyrosines, Tyr¹⁰⁷, Tyr²⁴⁴, and Tyr³⁰⁷. These residues are all conserved in the GH72 family, as well as several other residues lining the binding groove (Fig. 1A and Fig. 2). Together, the two laminaripentaose molecules appear to occupy the -5 to -1 and $+1$ to $+5$ binding sites, without any evidence of bond formation between the $-1/+1$ sugars, but with the -1 O-1 and $+1$ O-3 hydroxyls only 4.3 Å apart. Thus, this arrangement may represent the position of transglycosylation reactants, with the -5 to -1 sugars representing the donor site, and the $+1$ to $+5$ sugars representing the acceptor site.

The functions of the two catalytic residues, Glu¹⁷⁶ and Glu²⁷⁵, can be inferred from the ScGas2-laminaripentaose complex (Fig. 2). Glu¹⁷⁶, the catalytic acid/base, hydrogen bonds O-3 of the $+1$ sugar in the acceptor site, occupying a position equivalent to the catalytic base (Glu⁸⁹) in the PttXET16A structure (Fig. 2) (44). Glu²⁷⁵, on the opposite side of the binding groove, approaches the anomeric carbon of the -1 sugar to within 4 Å under a geometry compatible with nucleophilic attack. Mutation of either of these glutamates to glutamine abrogates catalytic activity (Table 2 and Fig. 3). GH families can be classified as inverting or retaining enzymes based on the distance between the two catalytic residues, with inverting enzymes giving a distance of 10 ± 2 Å on average, although retaining enzymes have the two residues located ~ 5.5 Å apart (45). In the ScGas2 crystal structure, Glu¹⁷⁶ and Glu²⁷⁵ are 5.1 Å apart, suggesting the active site structure is compatible with a retaining mechanism, in agreement with previously published product analysis of ScGas2 (21). Given the sequence conservation of these residues, this will extend to all GH72 members. In addition to the two glutamates, there are three conserved tyrosines lining the active site. Two of these (Tyr¹⁰⁷/Tyr²⁴⁴) interact with Glu²⁷⁵, positioning it for nucleophilic attack (Fig. 2). Mutation of these residues to phenylalanines shows small effects on hydrolysis (Table 2 and Fig. 3). A plethora of further interactions between protein and substrate is found in the elongated binding groove, involving both hydrogen bonds and stacking interactions with aromatic residues (Fig. 2). For instance, two conserved residues, Tyr¹⁰⁷ and Pro¹³⁶, are involved in hydrophobic stacking interactions with sugars in the donor site, whereas the conserved Arg¹⁴² gives the donor site a groove-like character (Fig. 2). Residues Asn¹⁷⁵ and

FIGURE 3. High pressure liquid chromatography analysis of $\beta(1,3)$ glucanosyltransferase/hydrolysis products. A, comparison of wild type ScGas2 kinetics against laminaripentaose and laminariheptaose, identifying laminaritetraose and laminaritriose as the main two degradation products of hydrolyzed laminariheptaose. B, product analysis from the incubation of the recombinant wild type ScGas2 and the following single mutant enzymes, Y107F, Y244Q, E275Q, and Y307Q, with 4 mM reduced G19 samples taken at the indicated time points.

Tyr³⁰⁷ hydrogen bond the -1 sugar, and mutation of these severely to moderately affects hydrolysis and transglycosylation, respectively (Table 2 and Fig. 3). Negative control mutations of residues that do not directly interact with the sugars (Gln⁶² and Asp¹³²) do not show significant effects on activity (Table 2 and Fig. 3).

Product Binding as a “Base Occlusion” Mechanism to Protect against Hydrolysis—The *ScGas2*-laminaripentaose complex suggests that it is possible for both products of the initial step in hydrolysis/transglycosylation to remain associated with the enzyme, with an “occlusion” of the catalytic base by the product in the acceptor site, very similar to what has been observed for the PttXET16A-acceptor complex (Fig. 2). This suggests that the enzyme may use binding of products from the initial step to protect the newly formed enzyme-sugar intermediate from nucleophilic attack by a water molecule. The products can then only be displaced by longer (and tighter binding) oligosaccharides, perhaps involving an acceptor-induced conformational change as suggested by Hartland *et al.* (21).

We sought to gain further support for this base occlusion hypothesis through soaking studies with a laminarioligosaccharide that is a substrate for hydrolysis, yet cannot act as both a donor and acceptor. We identified laminariheptaose as a suitable substrate for hydrolysis (yielding trimers and tetramers), without any measurable transglycosylation activity (Fig. 3A). Strikingly, soaking experiments with laminariheptaose resulted in electron density revealing that the oligosaccharide was hydrolyzed by the enzyme, leaving laminaritetraose in the donor site and laminaritriose in the acceptor site, in agreement with the kinetic data (Fig. 2 and Fig. 3A). The active site conformation is essentially identical to the laminaripentaose complex, but although the laminaritetraose occupies the -4 to -1 subsites, surprisingly on the acceptor side the laminaritriose occupies sites $+2$ to $+4$ (0.75 \AA maximum atomic shift with respect to the sugars in the laminaripentaose complex). Crucially, this leaves the $+1$ subsite, and thus the catalytic base, solvent-exposed. This allows for two important observations. First, the fact that laminaritriose, one of the hydrolysis products, occupies the $+2$ to $+4$ subsites, and not the $+1$ to $+3$ subsites, suggests that the leaving group of the initial nucleophilic attack can “slide” along the reducing end subsites, rather than randomly diffuse out of the active site. This may offer a transglycosylation mechanism with progressive exposure of subsites by a sliding out product with simultaneous occupation of these subsites by a new acceptor, while limiting access of water molecules near the covalent intermediate. Second, the observed arrangement in the acceptor side is in good agreement with the base occlusion model. Because the leaving group of the initial reaction with laminariheptaose moves to occupy the $+2$ to $+4$ subsites, this leaves the $+1$ subsite and the catalytic base fully exposed, allowing water to flood in, interact with the base, and act as a nucleophile to break the protein-enzyme intermediate, explaining why exclusively hydrolysis, and not transglycosylation, is observed with laminariheptaose (Fig. 3A). Indeed, an ordered water molecule ($B = 35 \text{ \AA}^2$) is seen to occupy a position in the -1 subsite in the laminariheptaose product complex, forming a hydrogen bond with the catalytic base (Fig. 2).

The base occlusion hypothesis also suggests that if interactions between the $+1$ sugar and the protein are disrupted, this might shift the balance between hydrolysis and transglycosylation away from the latter. We attempted this by studying the effects on hydrolysis and transglycosylation of a mutant (Y244F) of a conserved tyrosine lining the $+1$ subsite (Figs. 2 and 3 and Table 2). Strikingly, although hydrolysis is only moderately affected, a 10-fold reduction in transglycosylation is observed.

Concluding Remarks—Cell wall remodeling is an essential process in fungal organisms. Several enzymes with transglycosylation activities have been proposed to be involved in this process, but only the GH72 enzymes have been shown *in vitro* to transglycosylate the main cell wall carbohydrate polymer, $\beta(1,3)$ glucan (13, 14, 21). Genetic data in different organisms show the involvement of these enzymes in virulence, morphology, and growth, in some cases supporting an essential function in sporulation (12, 15, 17–20, 46).

Enzymes displaying significant transglycosylation are essentially glycoside hydrolases that have developed mechanisms to protect the (covalent) reaction intermediate from nucleophilic attack by a water molecule, although these mechanisms are not understood. The first crystal structure of a GH72 transglycosylase enzyme described here shows two interacting domains and a wide, conserved, and solvent-exposed active site. This includes the first crystal structure of an ordered CBM43 domain, which, although defining the CBM43 fold, does not immediately offer clues as to how it might contribute to glucan binding/hydrolysis/transglycosylation, as either truncation of the domain, or mutation of exposed aromatic residues does not have large effects on activity on (short) substrates.

Although recent work on xylosyltransferases has defined acceptor-protein interactions and has demonstrated that the donor-enzyme intermediate, generated after the initial nucleophilic attack, is long lived, this did not yet explain how transglycosylases might protect the intermediate from nucleophilic attack by water. The data described here provide the first insights into the mechanisms that may control the balance between hydrolysis and transglycosylation in a transglycosylase. The substrate-product trapped complexes, together with the mutagenesis data, suggest that product binding in the acceptor subsite might offer a method for occluding the catalytic base, and therefore prevent activation of an incoming water molecule. Compatible with this hypothesis, a substrate that yields a product that does not occupy the $+1$ site (leaving the catalytic base accessible to solvent), exclusively shows hydrolysis.

The fungal cell wall has been thought to be a treasure trove for novel drug targets to combat the increasing occurrence of invasive fungal infections. Indeed, the most recently developed anti-fungals of the echinocandin class target glucan synthase (1, 47), and there are efforts to develop inhibitors of fungal chitinases with anti-fungal activity (48, 49). Significant genetic validation now exists for the GH72 enzymes; they appear to be essential for proper development and morphogenesis of the fungal cell. Given the significant degree of sequence conservation in the GH72 family, it may be possible to develop chemical tools/probes that would inhibit all of the members of this mul-

tigene family in a single organism. The work here provides a useful scaffold for the future development and/or evaluation of such molecules.

Acknowledgments—We thank the European Synchrotron Radiation Facility, Grenoble, France, and Diamond Light Source, Oxford, United Kingdom, for beam time.

REFERENCES

- Latge, J. P. (2007) *Mol. Microbiol.* **66**, 279–290
- Fleet, G. H. (1991) in *The Yeasts* (Rose, A. H., ed) pp. 199–277, Academic Press, London
- Kollar, R., Petrakova, E., Ashwell, G., Robbins, P. W., and Cabib, E. (1995) *J. Biol. Chem.* **270**, 1170–1178
- Fontaine, T., Simenel, C., Dubreucq, G., Adam, O., Delepierre, M., Lemoine, J., Vorgias, C. E., Diaquin, M., and Latge, J. P. (2000) *J. Biol. Chem.* **275**, 27594–27607; Correction (2000) *J. Biol. Chem.* **275**, 41528
- Adams, D. J. (2004) *Microbiology* **150**, 2029–2035
- Mouyna, I., Fontaine, T., Vai, M., Monod, M., Fonzi, W. A., Diaquin, M., Popolo, L., Hartland, R. P., and Latge, J. P. (2000) *J. Biol. Chem.* **275**, 14882–14889
- Rodriguez-Pena, J. M., Cid, V. J., Arroyo, J., and Nombela, C. (2000) *Mol. Cell. Biol.* **20**, 3245–3255
- Kitagaki, H., Wu, H., Shimoi, H., and Ito, K. (2002) *Mol. Microbiol.* **46**, 1011–1022
- Tougan, T., Chiba, Y., Kakihara, Y., Hirata, A., and Nojima, H. (2002) *Genes Cells* **7**, 217–231
- Cabib, E., Blanco, N., Grau, C., Rodriguez-Pena, J. M., and Arroyo, J. (2007) *Mol. Microbiol.* **63**, 921–935
- Coutinho, P. M., and Henrissat, B. (1999) in *Recent Advances in Carbohydrate Bioengineering* (Gilbert, H. J., Davies, G., Henrissat, B., and Svensson, B., eds) pp. 3–12, Royal Society of Chemistry, Cambridge, UK
- Mouyna, I., Morelle, W., Vai, M., Monod, M., Lechenne, B., Fontaine, T., Beauvais, A., Sarfati, J., Prevost, M. C., Henry, C., and Latge, J. P. (2005) *Mol. Microbiol.* **56**, 1675–1688
- Mouyna, I., Monod, M., Fontaine, T., Henrissat, B., Lechenne, B., and Latge, J. P. (2000) *Biochem. J.* **347**, 741–747
- Ragni, E., Fontaine, T., Gissi, C., Latge, J. P., and Popolo, L. (2007) *Yeast* **24**, 297–308
- Ragni, E., Coluccio, A., Rolli, E., Rodriguez-Pena, J. M., Colasante, G., Arroyo, J., Neiman, A. M., and Popolo, L. (2007) *Eukaryot. Cell* **6**, 302–316
- Popolo, L., Vai, M., Gatti, E., Porello, S., Bonfante, P., Balestrini, R., and Alberghina, L. (1993) *J. Bacteriol.* **175**, 1879–1885
- Ram, A. F., Kapteyn, J. C., Montijn, R. C., Caro, L. H., Douwes, J. E., Baginsky, W., Mazur, P., van den Ende, H., and Klis, F. M. (1998) *J. Bacteriol.* **180**, 1418–1424
- Saporito-Irwin, S. M., Birse, C. E., Sypher, P. S., and Fonzi, W. A. (1995) *Mol. Cell. Biol.* **15**, 601–613
- Ghannoum, M. A., Spellberg, B., Saporito-Irwin, S. M., and Fonzi, W. A. (1995) *Infect. Immun.* **63**, 4528–4530
- Muhlschlegel, F. A., and Fonzi, W. A. (1997) *Mol. Cell. Biol.* **17**, 5960–5967
- Hartland, R. P., Fontaine, T., Debeaupuis, J. P., Simenel, C., Delepierre, M., and Latge, J. P. (1996) *J. Biol. Chem.* **271**, 26843–26849
- Otwinowski, Z., and Minor, W. (1997) *Methods Enzymol.* **276**, 307–326
- Collaborative Computational Project, No. 4 (1994) *Acta Crystallogr. Sect. D Biol. Crystallogr.* **50**, 760–763
- Pape, D., Seil, R., Kohn, D., and Schneider, G. (2004) *Orthop. Clin. North Am.* **35**, 293–303, viii
- Perrakis, A., Morris, R., and Lamzin, V. S. (1999) *Nat. Struct. Biol.* **6**, 458–463
- Emsley, P., and Cowtan, K. (2004) *Acta Crystallogr. Sect. D Biol. Crystallogr.* **60**, 2126–2132
- Murshudov, G. N., Vagin, A. A., and Dodson, E. J. (1997) *Acta Crystallogr. Sect. D Biol. Crystallogr.* **53**, 240–255
- Schuttelkopf, A. W., and van Aalten, D. M. (2004) *Acta Crystallogr. Sect. D Biol. Crystallogr.* **60**, 1355–1363
- Laskowski, R. A., Moss, D. S., and Thornton, J. M. (1993) *J. Mol. Biol.* **231**, 1049–1067
- Hoof, R. W., Vriend, G., Sander, C., and Abola, E. E. (1996) *Nature* **381**, 272
- Wierenga, R. K. (2001) *FEBS Lett.* **492**, 193–198
- Holm, L., and Sander, C. (1995) *Trends Biochem. Sci.* **20**, 478–480
- Jain, S., Drendel, W. B., Chen, Z. W., Mathews, F. S., Sly, W. S., and Grubb, J. H. (1996) *Nat. Struct. Biol.* **3**, 375–381
- Dias, F. M., Vincent, F., Pell, G., Prates, J. A., Centeno, M. S., Tailford, L. E., Ferreira, L. M., Fontes, C. M., Davies, G. J., and Gilbert, H. J. (2004) *J. Biol. Chem.* **279**, 25517–25526
- Popolo, L., Ragni, E., Carotti, C., Palomares, O., Aardema, R., Back, J. W., Dekker, H. L., de Koning, L. J., de Jong, L., and de Koster, C. G. (2008) *J. Biol. Chem.* **283**, 18553–18565
- Boraston, A. B., Bolam, D. N., Gilbert, H. J., and Davies, G. J. (2004) *Biochem. J.* **382**, 769–781
- Barral, P., Suarez, C., Batanero, E., Alfonso, C., Alche Jde, D., Rodriguez-Garcia, M. I., Villalba, M., Rivas, G., and Rodriguez, R. (2005) *Biochem. J.* **390**, 77–84
- Rodriguez, R., Villalba, M., Batanero, E., Palomares, O., Quiralte, J., Salamanca, G., Sirvent, S., Castro, L., and Prado, N. (2007) *J. Invest. Allergol. Clin. Immunol.* **17**, Suppl. 1, 4–10
- Trevino, M. A., Palomares, O., Castrillo, I., Villalba, M., Rodriguez, R., Rico, M., Santoro, J., and Bruix, M. (2008) *Protein Sci.* **17**, 371–376
- Shoseyov, O., Shani, Z., and Levy, I. (2006) *Microbiol. Mol. Biol. Rev.* **70**, 283–295
- Bahadur, R. P., Chakrabarti, P., Rodier, F., and Janin, J. (2003) *Proteins* **53**, 708–719
- Sulova, Z., Takacova, M., Steele, N. M., Fry, S. C., and Farkas, V. (1998) *Biochem. J.* **330**, 1475–1480
- Sulová, Z., Baran, R., and Farkas, V. (2001) *Plant Physiol. Biochem.* **39**, 927–932
- Johansson, P., Brumer, H., III, Baumann, M. J., Kallas, A. M., Henriksson, H., Denman, S. E., Teeri, T. T., and Jones, T. A. (2004) *Plant Cell* **16**, 874–886
- Rye, C. S., and Withers, S. G. (2000) *Curr. Opin. Chem. Biol.* **4**, 573–580
- de Medina-Redondo, M., Arnaiz-Pita, Y., Fontaine, T., Del Rey, F., Latge, J. P., and Vazquez de Aldana, C. R. (2008) *Mol. Microbiol.* **68**, 1283–1299
- Kauffman, C. A., and Carver, P. L. (2008) *Semin. Respir. Crit. Care Med.* **29**, 211–219
- Hurtado-Guerrero, R., and van Aalten, D. M. (2007) *Chem. Biol.* **14**, 589–599
- Andersen, O. A., Nathubhai, A., Dixon, M. J., Eggleston, I. M., and van Aalten, D. M. (2008) *Chem. Biol.* **15**, 295–301
- Bond, C. S. (2003) *Bioinformatics (Oxf)* **19**, 311–312